European Conference on Multifunctional Structures
EMuS 2020
Dr. J. Kos, Prof. X. Martinez and Dr. H. Schippers (Eds)

RF ANALYSES OF INTEGRATED KU-BAND ANTENNA EMUS 2020

J. VERPOORTE*, A. HULZINGA*,

M. MARTINEZ VÁZQUEZ†, J. LEISS†, M. WILLEMSEN†,

* Royal Netherlands Aerospace Centre (NLR)
Voorsterweg 31, 8316 PR Marknesse, The Netherlands
e-mail: {Jaco.Verpoorte, Adriaan.Hulzinga}@nlr.nl, web page: http://www.nlr.nl

† IMST GmbH
Carl-Friedrich-Gauss-Str. 2-4, 47475 Kamp-Lintfort, Germany
e-mail: {Martinez, Leiss, Willemsen}@imst.de, web page: http://www.imst.de

Key words: Phased array antenna, integration, simulation, measurement.

Abstract. In the ACASIAS project an integrated antenna for Ku-band satellite communication has been developed. The design of this integrated antenna has to meet structural, electromagnetic and thermal requirements. This paper addresses the electromagnetic performance of the antenna both by design and by measurement. For the design of the antenna, the electromagnetic interaction of the antenna with the conducting Carbon Fibre Reinforced Plastic (CFRP) ribs of the orthogrid and the interaction with the Glass Fibre Reinforced Plastic (GFRP) skin of the panel have been analysed. In addition, the influence of potential lightning diverters on the antenna performance has been analysed. The radiation pattern of a single antenna tile and the radiation pattern of an antenna tile integrated in the orthogrid fuselage panel were measured. The results of the antenna measurements are compared with the results of the simulations carried out for the design of the antenna.

1 INTRODUCTION

The ACASIAS project focuses on four innovative solutions, which aim at reduction of fuel consumption and reduction of CO_2 and NO_x emissions. One of these innovations concerns the integration of a Ku-band antenna array in the fuselage of the aircraft. The integrated Ku-band antenna will enable airborne satellite communication. The antenna array consists of 24 antenna tiles, which will be fully integrated in an orthogrid fuselage panel. The design bandwidth of the antenna is 2 GHz for the RX (receive) antenna and 0.5 GHz for the TX (transmit) antenna. The antenna elements consist of stacked patches to obtain this bandwidth. The design of this integrated antenna has to meet structural, electromagnetic and thermal requirements. This paper addresses the electromagnetic performance of the antenna both by design and by measurement.

For the design of the antenna, the electromagnetic interaction of the antenna with the conducting CFRP ribs of the orthogrid and the interaction with GFRP skin of the panel were analysed [1,2]. In addition, the influence of potential lightning diverters on the antenna performance was determined. The demonstrator antenna array will consist of 2 TX tiles

combined with 22 dummy tiles or 2 RX tiles combined with 22 dummy tiles. The TX and RX antenna tiles each consist of 8x8 antenna elements. Manufacturing of a full array of 24 active tiles was not possible in the scope of this project because of significant costs of the hardware. The dummy tiles are being used to investigate the thermal control of a full array of 24 tiles. The dummy tiles have the same thermal characteristics as the TX tiles. The antenna does not have a beamsteering network because the focus of the research was primarily on the integration aspects (electromagnetic interaction, thermal control). The antenna tiles were manufactured and afterwards subjected to electromagnetic and thermal tests. The electromagnetic tests comprise measurement of the radiation patterns. The radiation pattern of a single antenna tile and the radiation pattern of an antenna tile integrated in the orthogrid fuselage panel were measured. In this paper the results of the antenna measurements are compared with the results of the simulations carried out for the design of the antenna.

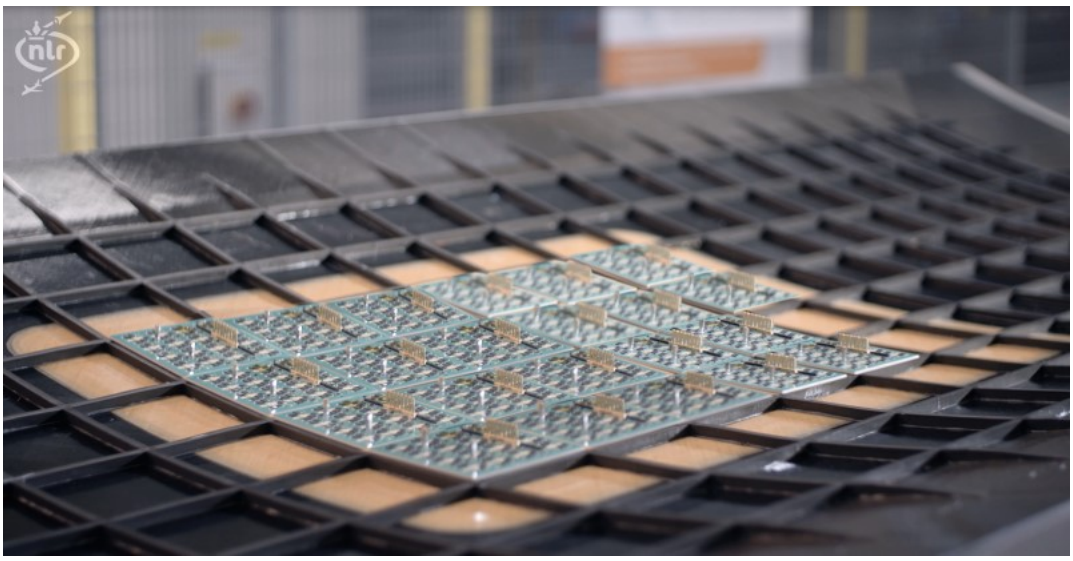

Figure 1: Ku-band antenna tiles integrated in a full-scale fuselage panel consisting of a CFRP orthogrid. The skin of the panel is also made of CFRP but in the center of the panel the skin is made of GFRP which is transparent for the electromagnetic waves.

2 SIMULATION OF INTEGRATED ANTENNA PERFORMANCE

For the design of the integrated antenna array several simulations were carried out to assess the influence of the orthogrid and skin on the antenna performance (the input impedance and radiation pattern). Also the potential influence of lightning diverters was assessed.

2.1 Influence of CFRP orthogrid and GFRP skin

The radiation patterns of a single antenna tile (non-integrated and integrated) are shown in Figure 2 and Figure 3. These patterns were calculated by using EMPIRE XPU™. The 8x8 array has a null-to-null beamwidth of about 28° and a first sidelobe level at -13.5 dB as expected for a rectangular array of 8x8 antenna elements with uniform amplitude distribution. The cross-polarization level is about -16 dB. Figure 3 shows the effect of integrating the

antenna in a conductive orthogrid with GFRP skin. For this simulation the distance between antenna tile and GFRP skin was 6 mm. The simulations show a reduced level of the sidelobes, for both co-polar and cross-polar. The effect on the main lobe is not significant.

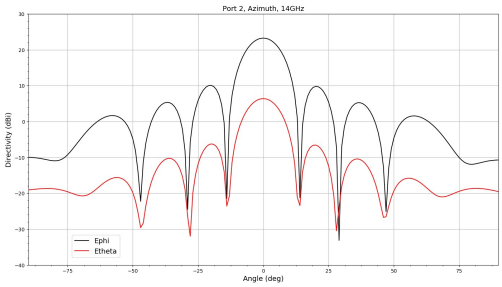

Figure 2: Radiation pattern of a single antenna tile (polarization 2, azimuth scan at 14 GHz).

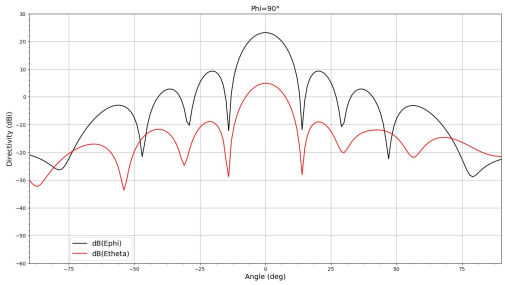

Figure 3: Radiation pattern of an integrated antenna tile (polarization 2, azimuth scan at 14 GHz) for 6 mm distance between the antenna tile and the skin.

In [1] and [2] the influence of the tile separation on the radiation pattern was described. The antenna tiles have a separation of 7 mm due to the thickness of the ribs of the orthogrid. This separation is in the order of a quarter of the wavelength and therefore this gap will have an influence on the radiation pattern. Due to the tile separation there is an increase in sidelobes (Figure 4). In order to comply with limits for the radiation pattern of transmit antennas for Ku-band satellite communication [4][5], these sidelobes will have to be suppressed. This can be done applying amplitude tapering to the array. However, this will add additional complexity and the overall efficiency of the antenna will decrease.

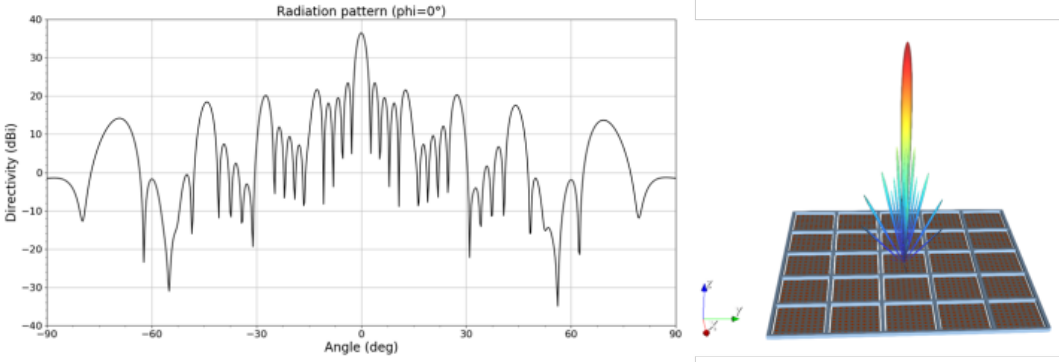

Figure 4: Radiation pattern of the full 40*40 elements array (gap between 8*8 tiles: 7 mm).

The influence of the thickness of the GFRP skin was also addressed in [1]. For structural strength and stiffness purposes the GFRP skin thickness has a thickness of 2.1 mm. This is not ideal for electromagnetic purposes. Either a thin (1 mm or less) or a half-wavelength thick skin would be the most optimum.

In addition the distance of the tile to the skin is of influence on the antenna performance. Simulations have shown that, to minimize the influence of the skin on the input impedance of the antenna elements, the antenna should have a certain minimum distance to the skin (in the order of 6 mm). This behavior is confirmed by measurements (section 3.1).

2.2 Influence of metal lightning diverters

The antenna array will have lightning protection on two levels: for protection against direct lightning effects lightning diverter strips will be used and for protection against indirect lightning effects the top patch of the stacked patch antenna elements will be grounded (this also protects against electrostatic discharge). The lightning diverter strips will be installed only above the ribs of the orthogrid in order not to disturb the radiation pattern of the antenna tiles. The analysis described in [1] showed that the influence of the lightning diverters is visible but the effect is negligible and the radiation pattern is still acceptable.

3 MEASUREMENT OF INTEGRATED ANTENNA PERFORMANCE

3.1 Influence of CFRP orthogrid and GFRP skin

To assess the influence of the orthogrid and skin on the antenna performance, radiation pattern measurements were carried out on a single TX antenna integrated in an aluminium orthogrid with GFRP skin (Figure 5). The aluminium ribs of the orthogrid are more conductive than the CFRP ribs of the full-scale fuselage panel but the influence on the antenna performance is similar.

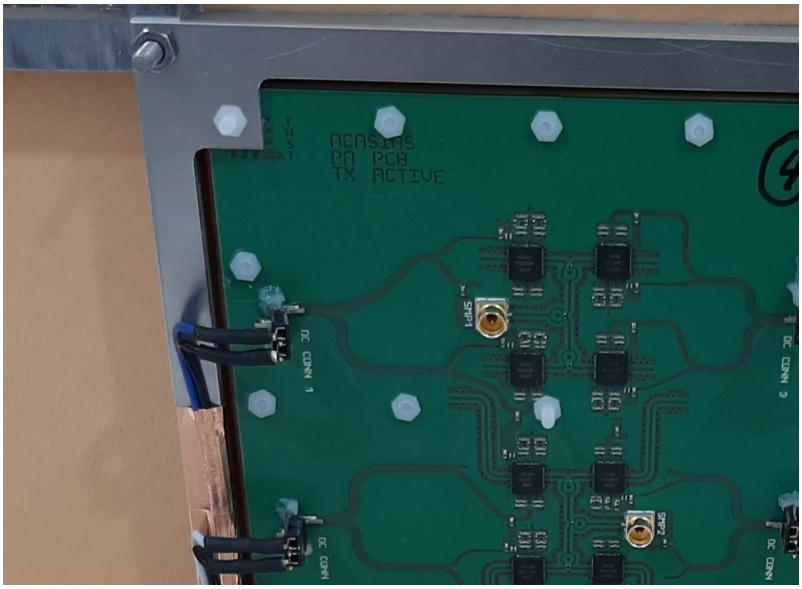

Figure 5: Single TX antenna tile integrated in aluminium orthogrid with GFRP skin.

The results of the measurements are shown in Figure 6 and Figure 7. The figures show the measured antenna gain normalized to the gain of the non-integrated antenna tile at 14 GHz. Measurements were carried out with and without orthogrid. In addition the distance between the antenna tile and the skin was varied by using a metal bracket. The results of the co-polar measurements of a single linear polarization are shown in Figure 6 for several distances between skin and antenna tile. The distance between the skin and the tile has a significant influence on the received power. The highest gain of an integrated antenna tile is achieved for

a distance of 6 mm. At that distance the gain is about the same as for the antenna tile which is not integrated. For shorter distances the gain decreases and the sidelobes increase. The sidelobe level for the case of the non-integrated antenna is higher than predicted (-7 dB versus -13.5 dB). This is probably caused by small differences between the amplifiers, splitters and traces used in the antenna. In the simulations ideal components were used.

Figure 7 shows the results of the co-polar and cross-polar measurements of the TX antenna tile integrated in the panel (with a distance of 6 mm to the skin). In the main lobe the ratio between the co-polarization and the cross-polarization is about 15 dB. This is close to the predicted level.

As soon as the RX tiles are available, the same measurements will be carried out on the RX tiles as on the TX tiles. It is expected that the behavior of the RX tiles is similar to the that of the TX tiles. Finally, also the thermal behavior of the integrated tiles will be measured.

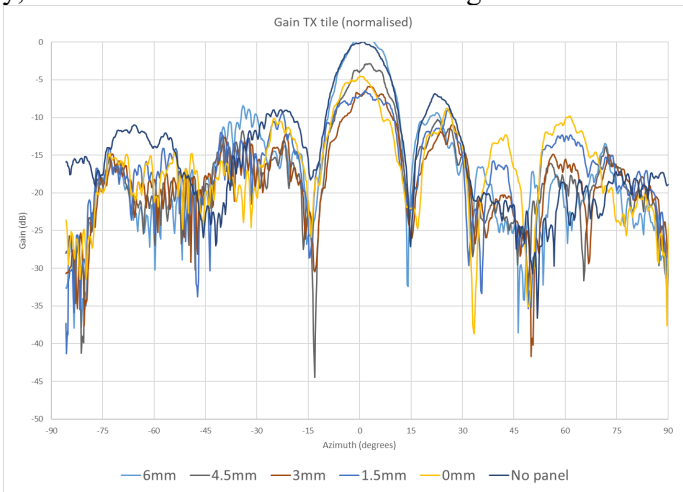

Figure 6: Normalised antenna gain of TX tile (measured) for several distances between the skin and the tile aperture and for the case of a single antenna not integrated in the fuselage panel.

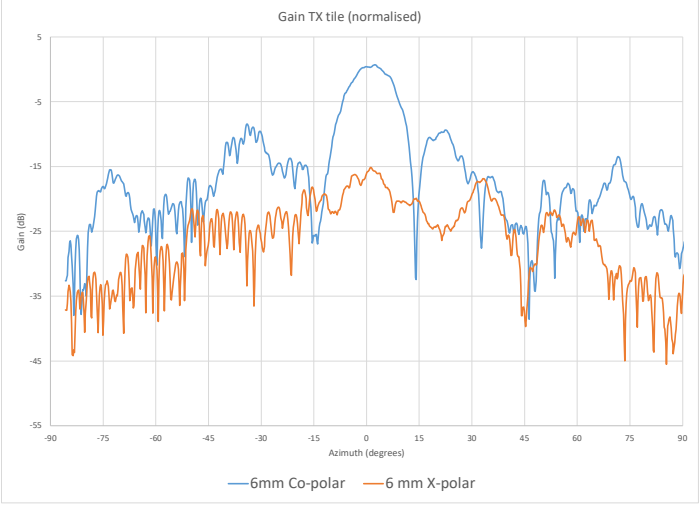

Figure 7: Normalised antenna gain of TX tile (measured) for co-polarisation and cross-polarisation. In both cases the distance between the antenna tile and the skin is 6 mm.

4 CONCLUSIONS

During the design of the integrated antenna tile the influence of the CFRP orthogrid and GFRP skin on the antenna performance was analyzed. The orthogrid and skin have an influence on the performance of the antenna but the effects are either acceptable or can be compensated (application of tapering to reduce sidelobe level). The effect on the antenna performance of lightning diverters added to the skin of the panel is negligible. The measurements on an integrated antenna tile confirm the influence of the GFRP skin. The best antenna performance is obtained for a distance of 6 mm between antenna and skin. The measurements on an integrated antenna tile confirm the predicted ratio between the co-polar and the cross-polar level in the main beam. The measurements show that integration of a Ku-band antenna tile in a composite structure is feasible without significant loss of performance.

ACKNOWLEDGMENT

All work described in this paper has received funding from the European Union's Horizon 2020 research and innovation programme under grant agreement No. 723167, ACASIAS project. The authors want to acknowledge the contribution of all the partners in the ACASIAS project.

REFERENCES

[1] "Structural Integration of Ku-band SatCom Antenna into novel Fuselage Panel", J. Verpoorte and A. Hulzinga, EMuS 2019 Conference.

[2] "Advanced Concepts for Aero-Structures with Integrated Antennas and Sensors (ACASIAS)", Yuri Konter, Jaco Verpoorte, Adriaan Hulzinga, Marta Martínez Vázquez, ESA Antenna Workshop 2019.

[3] "Structurally integrated phased array antennas for aeronautical SatCom applications", Marta Martínez-Vázquez, Jaco Verpoorte, Jens Leiß, Maren Willemsen, Adriaan Hulzinga, Zdeněk Řezníček, submitted for EuCAP 2021.

[4] ITU recommendation S.1428-1 "Reference FSS earth-station radiation patterns for use in interference assessment involving non-GSO satellites in frequency bands between 10.7 GHz and 30 GHz"

[5] ETSI 302 186 "Harmonised Standard for satellite mobile Aircraft Earth Stations (AESs) operating in the 11/12/14 GHz frequency bands"